Chapter 16 Ephemeris and Clock Navigation Message Accuracy

J. F. Zumberge and W. 1. Bertiger

1 n this chapter we discuss the accuracy of the ephemeris and clock corrections contained in the GPS navigation message.. Wc. first provide a brie.f description of how the Control Segment generates these quantities. Next, we compare them with results from precise (non-rc:il-time) solutions of satellite parameters derived from the simultaneous analysis of data from a globally-distrib uted network of GPS receivers. Finally, wc cast these accuracies into the form of a user equivalent range error.

1. Control Segment Generation of Predicted Ephemerides and Clock Corrections

One of the primary purposes of the Control Segment (Chapter 1 ()) is to generate predicted satellite ephemerides and clock corrections, which arc regularly uploaded to the satellites. The predictions arc then included as part of the 50-bps 1 500-bit navigation message (Chapter 4) that modulates the transmitted GPS signs]. Ground receivers then use the predictions for rcdl-time estimates of satellite coordinates and clock corrections,

Data used for the predictions arc acquired from receivers situated at precisely known locations in Hawaii, Colorado, Ascension Island in the Atlantic Ocean, Diego Garcia in the northern Indian Ocean, and Kwajalein in the western Pacific. The distribution in longitude of the.sc sites (Table 1) is reasonably uniform, allowing continuous tracking of all GPS spacecraft. The sites at Ascension, Diego Garcia, and Kwajalein arc capable of transmitting computed navigation message updates to the satellites. Receivers at all stations use cesium oscillators for time stability, and m ea sure dual-frequ ency phase and p se udorange. Meteorological data arc acquired at each station and used to aid in estimation of troposphere delay. All data arc regularly transmitted to the Master Control Station in Colorado Springs.

Table 1 Tracking stations used by the Control Segment and approximate locations

site	latitude	longitude
Hawaii	21° N	158° W
Colorado Springs*	39° N	105° W
Ascension Island†	8° S	14° W
Diego Garcia†	7° S	72° E
Kwajalein†	9° N	168° E

*Master Control Station
†Can transmit to GPS satellites

Only the P-code p seudorange measurements are used as data in the p arameter estimation scheme, which is based on a Kalman filter. Estimated satellite parameters include epoch-state position and velocity, solar radiation pressure coefficients, clock bias, drift, and drift rate. Station parameters include similar clock quantities and troposheric delay. The terrestrial coordinate system and gravity field arc WGS84. The reference time is an average of monitor station clocks and a subset Of GPS clocks.

Data going back four weeks tire nominal l y used to cst imate satellite parameters, which are then used to predict sate.llitc positions and clock corrections into the future. The first 28

hours of prediction are divided into overlapping 4-hour intervals separated by one hour. The predictions for each such interval are cast in the format of the navigation message (through a fitting procedure), and arc uploaded into the satellites once a day, more frequently if required to meet a IO-meter user-equivalent range error specification. The daily upload is based on a data window which closed 45 minutes prior to the upload.

Given the daily upload, the satellite broadcasts satellite positions and clock corrections contained in the appropriate 4-hour interval. Although predictions beyond 28 hours are also uploaded, they arc normally not be used, as the next day's upload overwrites them with results derived from more current data.

2. Accuracy of the Navigation Message

It is the goal of this section to assess the accuracy of the information broadcast in the navigation message. The "truth cases" to which the navigation messages will bc.compared are daily GPS solutions, from the Jet Propulsion Laboratory (l]>].), of satellite positions and clock corrections. Fist wc describe the daily JPL solutions, including estimates of their accuracies. Next, base.ci on the period 1993 Jul 04 - Oct 22, we compare. these daily solutions with their counterparts from the navigation message.

2.1 Global Network GPS Analyis at the Jet Propulsion Laboratory

Since 1992 June, analysts at JPL have regularly reduced GPS data from a globally-distributed network of 20-40 precision P-code GPS receivers. Shown in Figure 1 are locations of the sites as of Fall 1993. in addition to dense coverage in North America and Europe, there is also reasonable coverage elsewhere, including eight sites in the Southern hemisphere.

Receivers at these sites make measurements of the carrier phase and pseudorange observables on both the 1.1 and 1.2 bands from GPS satellites, at a 30-second data interval. Data are analyzed daily in 30-hour batches, centered on GPS noon. The six-hour overlap centered at each GPS midnight allows for consistency checks between solutions from adjacent days. Prior to parameter estimation, data are edited using the TurboEdit alogrithm (Blewitt, 1990) and decimated to a 10-minute interval.

The model used in the analysis corrects for ionospheric delay (through the formation of the iol]os]>l)clc-flee linear combination of phase and pseudorange observables), tropospheric delay (by stochastic estimation of the wet component at each receiver site), transmitter and receiver phase center offsets, earth orientation (through explicit estimation of pole position and length of day), solid earth tides, and relativistic effects. Transmitter and receiver clock corrections are estimated as independent parameters at each sample lime. The reference clock is a hydrogen maser driving one of the receivers. Satellite parameters include epoch-state position and velocity, and solar radiation pressure; the latter is estimated stochastically. The earth-fixe(i reference frame is defined by adopting fixed locations for eight of the receivers as specified in the International Terrestrial Reference Frame, ITRF91 (Boucher *et al.*, 1992; Blewitt *et al.* 1992). The carrier phase biases are estimated as piecewise-constant real-vallIc(i parameters.

2.2 Accuracy of the Precise Solution

One assessment of orbit quality from the precise solutions can be made by looking at the continuity of results from adjacent days. For example, the solution for October 7 uses data

from 21:00 110111s on October 6 through 03:00 110111's 011 October 8. similarly, the solution for October 6 uses data from 21:00 hours on October 5 through 03:00 hours on October 7. The difference between these solutions in the position of prn I 2 within ±3 hours of midnight between October 6 and **7** is shown in Figure 2. The rms variation over the 6-hour period is 12 cm, 22 cm, and 25 cm for the radial, cross-track, and along-track components, respectively,

A number of other groups estimate sate.]]itc parameters from the same data, using independent software, thus allowing a separate assessment of orbit quality. Shown in Figure 3 is the comparison of JPI ,'s orbit solution for prn 12 on 1993 October 7 with that determined by the Center for Orbit Determination in Europe (CODE) at the Universit y of Berne, Switzerland. The vertical scale is the same as that in Figure 2. The root-mean-square difference over the day between the solutions is 7 cm for the dial component, 5 cm for the cross track, and 9 cm for the along track. For other days and satellites, this agreement is generally within 2,() cm for all components. Comparisons with results from other analysis centers show comparable agreement. '1'0 summarize, the precise orbit solutions are. typically accurate to 5-30 cm rms, depending on the component and other factors.

A comparison similar to that shown in Figure 2 is shown for a transmitter clock in Figure 4. Plotted there is the difference between the Oct 6 and Oct 7 solution for the prn 13 clock. The rms difference over the 6-hour period is ().22 nsec, of which a portion is due to a O. 1 8-nsec bias. This few-tenths-nscc rms difference is typical for other satellites and days,

The reference for the precise clock solutions is the maser-based receiver at Algonquin Park, Canada, maintained by the Geodetic Survey Division of Canada's Department of Energy, Mines and Resources. This clock is adjusted periodically, and is believed accurate with respect to GPS time to within a few hundred nsec, with drift magnitudes of no more than a few lens of nsec per day. Of course, biases and drifts in the reference clock will be masked in a comparison 1 ike 1 igure 4, but would appear in a comparison bet ween the navigation message and the precise solutions.

2.3 Comparison of Precise Orbits with Broadcast Ephemerides

Shown in Figure 5 is the position difference between the J']. precise solution and the broadcast orbit for prn 12 on 1993 October 7. The interval between updated navigation messages is typically one hour. The satellite and day are the same as in Figures 2 and 3, although the vertical scale is 10X larger. The rms values over the day are 0.56 m for the radial component, 1,67 m for the cross track, and 2,67 m for the along track.

Similar calculations have been made for all satellites and days over the period 1993 July 1 through 1993 October 2.2 (a total of 2490 sate.]]itc days), For the given satellite and day, the rms difference over the day between the broadcast ephemeris and the precise solution is computed, for each Of the three components . The results are summarized in Figure 6.

1 igure 6 contains three. histograms, one for each of the position difference components. The median val ues ill the above distributions arc. 1.3 m for the radial component, 3.6 for the cross track, and 4.7 m for the along track. Thus, half of the satellites and days over the ~4-month period had a daily rms agreement between the navigation message and the precise solution of less than 1.3 m in the radial component.

The reference frame ITRF91 used for the preci se solution s di ffers from WGS84, used b y the broadcast ephemeris. To test how much this reference-fr ame difference contributes to the observed difference in ephemerid es, consider the 7-parai neter transformation defined by

$$\mathbf{x}' = (1+\varepsilon)\,\mathbf{x} + \mathbf{t} + \Theta\,\mathbf{x}\ ,$$

where $\mathbf{t}$ is a translation vector, ε a scale factor, and

$$\Theta \equiv \begin{pmatrix} 0 & -0, & 0_y \\ 0_z & 0 & -0 \\ -0_y & 0x & 0 \end{pmatrix}$$

is a rotation matrix. The calculations which resulted in Figure 6 were repeated, but each day a transformation was applied to all coordinates in the broadcast message. The parameters were.chosen to minimize $\sum_{pct}[\Delta_{pct}^2]$ where $\Delta_{pct} \equiv X_{pct} - x'_{pct}$ is the difference at time t between the precise orbit (X_{pct}) and the transformed broadcast orbit (x'_{pct}) for prn p and Cartesian component c.

The median values of the daily rms differences in the radial, cross track, and along-track components are reduced to 1.2 111, 3.2 m, and 4.5 m, respectively, from the values corresponding to Figure 6 . The values of the transformation parameters are given in Table 2, and Figure 7 shows the daily values of the. scale factor.

Table 2 Parameters in the transformation from the WGS 84 reference frame to the International Terrestrial Reference Frame. The quantities are based on 120 daily transformations of navigation-message orbits into the precise orbits. (The uncertainties in the average values are based on observed daily fluctuations, shown in the third column, divided by $\sqrt{120}$.) The most significant parameters are the -12.7×10^{-9} scale factor and the -125.5-nrad rotation around the z-axis.

parameter	average	standard deviation
t_x (m)	-4.0±2.3	24.7
1, (cm)	6.321.8	19.6
t_z (cm)	-4.623.3	36.3
ε (ppb)	-12.7±0.2	2.'2
0_x (nrad)	-7.9±3.2	34.9
0_y (III-ad)	-6.823.3	35.9
0/ (m(l)	125.5±4.3	47.2

'1'here are two known effects which would contribute to the scale factor parameter ε. The first is **that the** precise orbits refer to the space.craft center of mass while the broadcast refer to the. spacecraft antenna phase **center. Because** these points are separated by 0.9519 meter, mostly in the radial direction, one could expect a contribution of about ().9519/(26.55 x 10^6) ≈ +35.9 ppb to ε in the broadcast-to-precise transformation.

Second, the broadcast orbits use the WGS84 gravity field, with $GM = 3.986005 \times 10^5\ km^3\ sec^{-2}$, **compared with the** JGM2 value (Nerem *et al.*) of 3.986004415 x $10^5\ km^3\ sec^{-2}$ used in the precise solutions. Because the radius varies with $(GM)^{1/3}$, we would expect a contribution to ε of

$$-\frac{1}{3}\left(\frac{3.986005 - 3.986004415}{3.986004415}\right) \approx -48.9 \text{ ppb.}$$

(The larger value of WGS84 would put the satellite out further, requiring a negative value of ε to bring it into agreement with the precise.) The sum of these expectations, - 13.1 ppb, is remarkably close to the value of - 12.7 ppb in Table 2.

The differences between the precise and broadcast orbits are significantly larger [ban the accuracies of the precise solutions, as estimated in the previous section. This is not surprising, as the broadcast solutions are by necessity the result of an extrapolation in time from hours-old data. The precise solutions, on the other hand, do not have such a real-time constraint.

It should also be mentioned that the intentional degradation of broadcast ephemeris quality, one speculated aspect of Selective Availability, has not been observed.

2.4 Comparison of Precise Clocks with Broadcast Clocks

Shown in Figure 8 are the the clock corrections for prn13 on 1993 October 7, as determined by J]'] .'s precise solution (solid squares) and that from the navigation message (opt.Jl Circle.s). The interval between points is 30 minutes. (Points whose estimated uncertainty - "formal error" - exceeds 1 () ns in the precise solution are not considered.) The difference between the navigation message and the. precise solution is shown in Figure 9, where the discontinuities in the former are clearly evident.

GPS satellites on this day can be grouped into two classes depending on the variation over the day in the difference between the precise. and broadcast clocks. Figures 9 and 1() contain satellites in the group for which this scatter is of the order of 10 nsec. Of the five satellites in this group, three are Block I (prn's 3, 12, and 13) and two are Block 11 (prn's 15 and 20). Note that the time. series in Figures 9 and 10 are reasonably smooth with time.

The second class consists of satellites for which the difference is much noisier. All satellites in this group are Block]], and are shown in Figure 11 as a function of time, together with the histogram that indicates the distribution Of the differences. The standard deviation of the distribution is about 80 ns.

The clock dithering component of Selective Availability is clearly evident in Ibis second class, and absent from the first class. Note that the biases of the distributions in Figures 9- 11 are all about -120 nsec, and thus represent a constant difference between GPS reference time and that of the precise solution. This could be entirely due to the maser-based reference clock used for' the latter.

Similar analyses of GPS clocks were made for all satellites and days from 1993 Jul 04 through 1993 Oct 22. For each day and satellite, any linear trend in the difference between the precise solution and the broadcast clock over the day was removed. The average difference in drift between the precise reference time. and the GPS reference time is - 20.1 ns/day. This difference can be seen, for example, in the plots of Figure 10.

The standard deviation over the day of the dc-trended difference has also been calculated. The distribution of daily standard deviations is shown in Figure 12. Note the. logarithmic scale on both axes. The median of the lower distribution is 4.5 nsec, which represents the accuracy of the broadcast clock correction for satellites not affected by clock dithering. The median of the upper distribution is 79.9 nsec. Thus clock dithering essentially limits the accuracy of the broadcast correction to this level.

Table 3 compares these results with a prediction (Russell and Schaibly, 1 980) of how well the GPS Control Segment would be able to predict clock corrections and GPS ephemerides. The prediction is reasonably consistent with the comparisons between the navigation message and the JPL precise solution, as discussed in this section.

One can cast these performances into a user- equivalent range error σ_u (Bernstein):

$$\sigma_u^2 = \sigma_r^2 + c^2 \sigma_t^2 + 2 \rho_{rt} \sigma_r c \sigma_t + k (\sigma_x^2 + \sigma_a^2)$$

where ρ_{rt} is the correlation coefficient between the radial and clock errors, c is the speed of light, and $k \approx 0.0192$. Shown in Table 4 are the contributions to σ_u, assuming that ρ_{rt} = (),31.

Table 3 GPS Control Segment Performance, Predicted and Observed

parameter	prediction	observed
radial (σ_r)	**0.8111**	1.2111
cross track (σ_x)	3.() m	3.2 m
along track (σ_a)	6.3111	4.5111
clock (no SA) (σ_t)	7.7 nsec	4.5 nsec
clock (w/ SA)		79.9 nsec

When SA clock dithering is not in effect, the contributions to σ_u from the ephemeris and clock errors are comparable, with a result of $\sigma_u \approx 2$ m. The more usual circumstance, however, has clock dithering in effect, in which case the by-far-dominant contribution to σ_u is from the 80-nsec noise in the broadcast clock, resulting in $\sigma_u \approx 24$ m.

Table 4 User Equivalent Range Error (meters)

	σ_r	$c\ \sigma_t$	$\sqrt{(2\ \sigma_r\ c\ \sigma_t)}$	$\sqrt{[k(\sigma_x^2 + \sigma_a^2)]}$	σ_u $\rho_{rt} = -1$	$\rho_{rt} = 0$	$\rho_{rt} = +1$
no SA	1.2	1.3	1.8	0.8	0.8	2.()	2.7
with SA	I .2	24.()	7.6	0.8	22.8	24.0	25.2

References

Bernstein, H., *Calculations of User Range Error (URE), Variance from a Global Positioning System (GPS) Satellite*, Aerospace Report No. TOR-0083 (3476-02)-1, 1983.

Boucher, C., Z. Altamimi, L. Duhem, IERS Technical Note 12, *ITRF 91 and its associated velocity field,* October 1992, Observatoire de Paris.

Blewitt, G., An automatic editing algorithm for GPS data, *Geophys. Res. Lett., 17,* (3), 199-202, 1990.

Blewitt, G., Michael B. Heflin, Frank H. Webb, Ulf J. Lindqwister, and Rajendra P. Malla, Global coordinates with centimeter accuracy in the International Terrestrial Reference Frame using GPS, *Geophys. Res. Lett., 19,* (9), 853-856, 1992.

Nerem, R. S., F. J. Lerch, J. A. Marshall, E. C. Pavlis, B. H. Putney, B. D. Tapley, R. J. Eanes, J. C. Ries, B. E. Schutz, C. K. Shum, M. M. Watkins, J. C. Chin, S. M. Klosko, S. B. Luthcke, G. B. Patel, N. K. Pavlis, R. G. Williamson, R. H. Rapp, R. Biancale, and F. Nouel, Gravity model development for TOPEX/Poseidon: Joint Gravity Models 1 and 2, *J. Geophys. Res.,* submitted, 1994.

Rusell, S. S. and J. H. Schaibly, "Control Segment and User Performance," *Global Positioning System, Papers published in* NAVIGATION, 1980, The Institute of Navigation.

David Wells *et al.*, *Guide to GPS Positioning*, 1986, Canadian GPS Associates, Fredericton, New Brunswick, Canada.

Figure 1 Global distribution of GPS tracking receivers, Fall 1993. in addition to dense coverage in North America and Europe, (here is also reasonable coverage elsewhere, including 8 sites in the southern hemisphere.

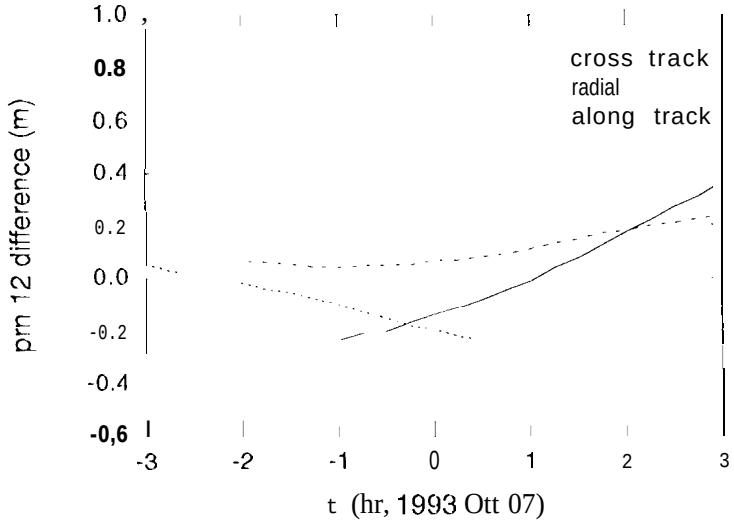

Figure 2 Difference near the midnight boundary between JPL's precise solutions of 1993 October 6 and October 7. The rms differences arc 0.12 m, ().22 In, and 0.25 m in the radial, cross-track, and along-track components.

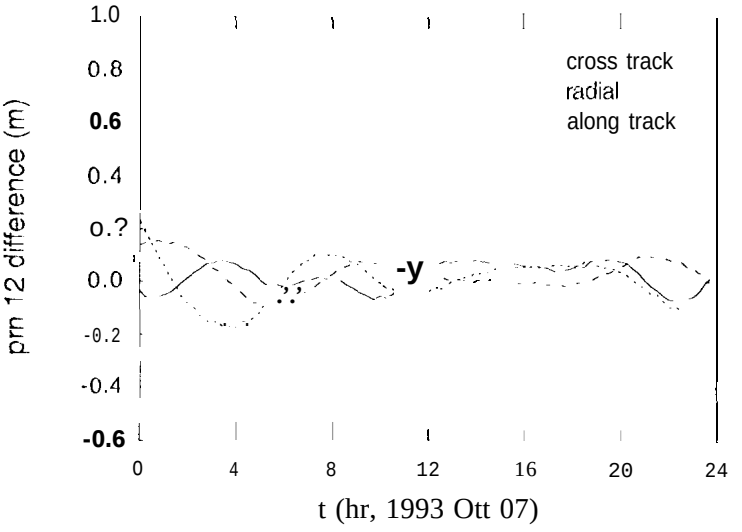

Figure 3 Comparison of the precise solution from JPI , with that from the CODE (University of Berne), for prn 12011 1993 Oct 7. The rms values over the day (which include both the bias and the variation) are ().()7 m for the radial component, 0.05 m 101" the cross track, and ().()9 m for the along track. The agreement between .1 PL and CODE for this satellite and day is somewhat better than typical. However, for other satellites and days the agreement is, with few exceptions, at least as good as a few tens of centimeters.

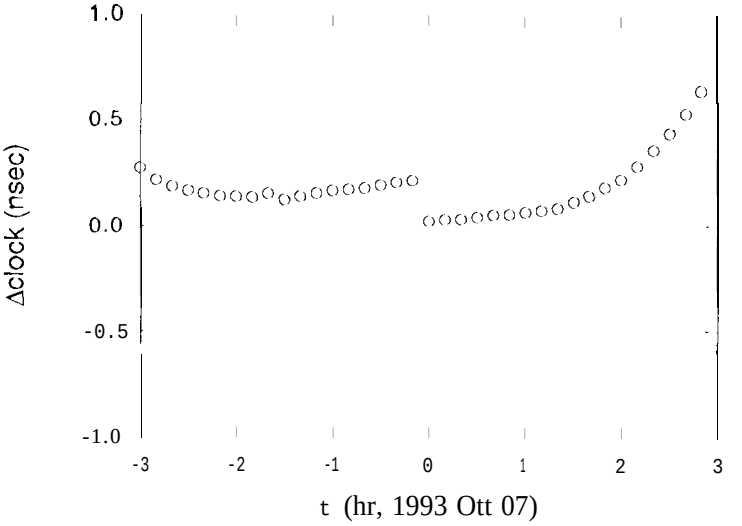

Figure 4 The difference in the clock solution for prn 13 from the 1993 Oct 06 solution and the 1993 Oct 07 solution. The rms value over the 6-hour overlap is ().22 nsec (of which a portion is due to a (). 1 8-nsec bias).

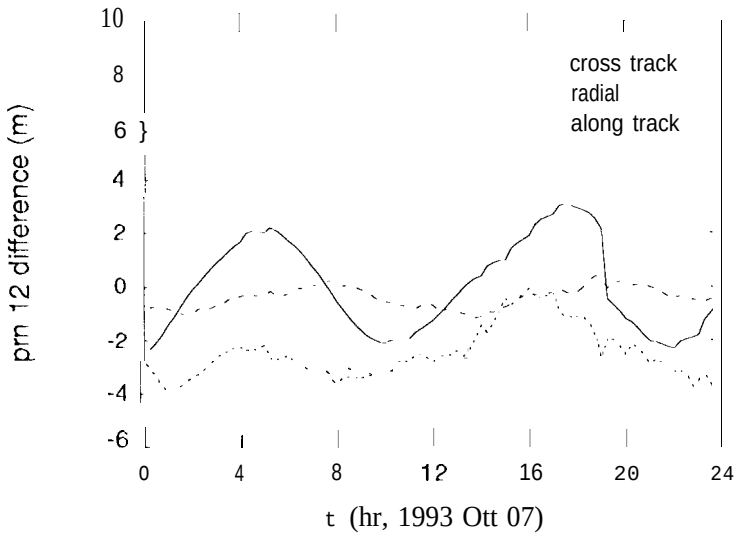

Figure 5 Comparison of the broadcast ephemeris with JPL's precise solution, for prn 12 on 1993 Oct 07. The rms values over the day are 0.56 m for the radial component, 1.67 m for the cross track, and **2.67** m for the along track. The vertical scale is 10× that of Figures 2 and 3.

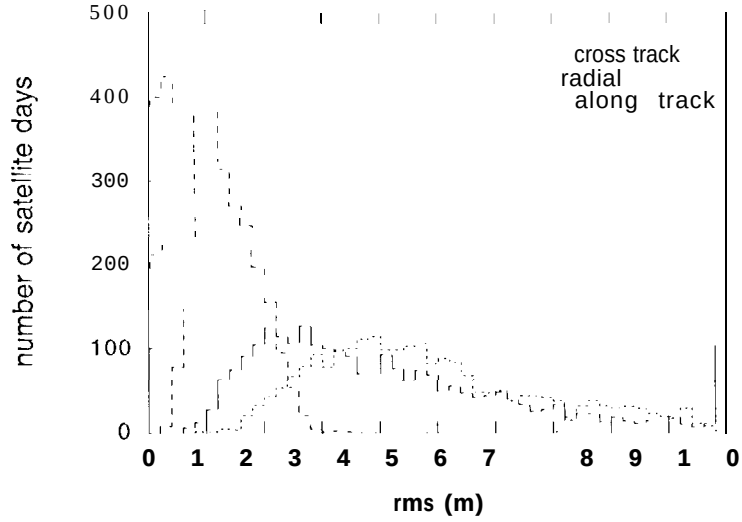

Figure 6 Comparison of the broadcast ephemeris with precise orbital solutions for the period 1993 Jul 04 through 1993 Oct 22. An "event" in one of the three histogram corresponds to a single satellite on a single day (as in Figure 5). For **the** given satellite and day, the rms difference over the day between the broadcast ephemeris and the precise solution is computed, for each of the three components. The median values in the above distributions are 1.3 m for the radial component, 3.6 for the cross track, and 4.7 m for the along track. If a daily 7-parameter transformation is applied to align the navigation message reference frame with that of the precise solution, the medians are marginally reduced to 1.2 m, 3.2 m, and 4.5 m.

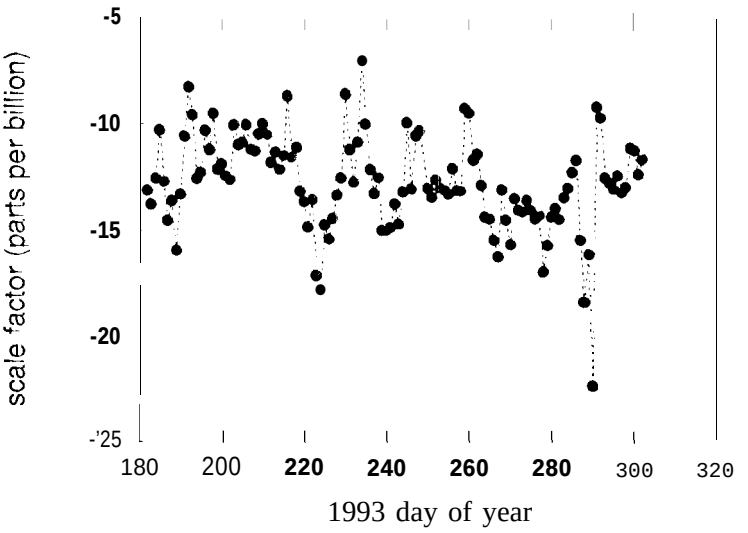

Figure 7 The scale factor in the transformation from the WGS 84 reference frame to the International Terrestrial Reference Frame. The average value is 12.7~ ().2 parts per billion, which corresponds to about -30 cm in the radial direction.

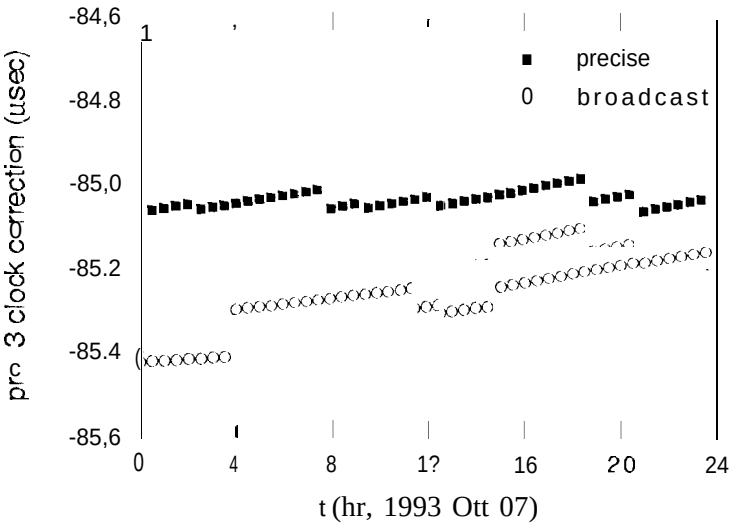

Figure 8 The clock correction for prn 13 broadcast in the navigation message (open circles) and determined in JPL's precise solution (solid squares). The precise solution uses a maser based GPS receiver as its reference. The solid squares describe a slope of about 250 ns/day.

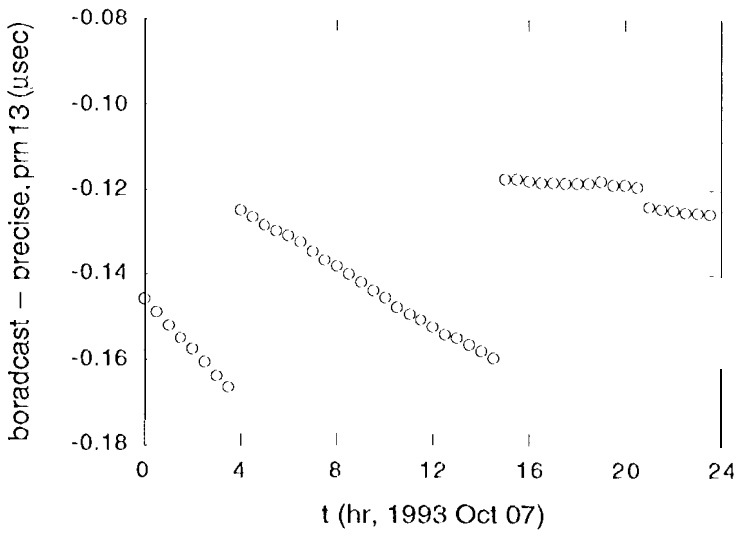

Figure 9 The difference in the broadcast and precise clock corrections for prn13. The discontinuities are due to new broadcast messages, as indicated in Figure 8.

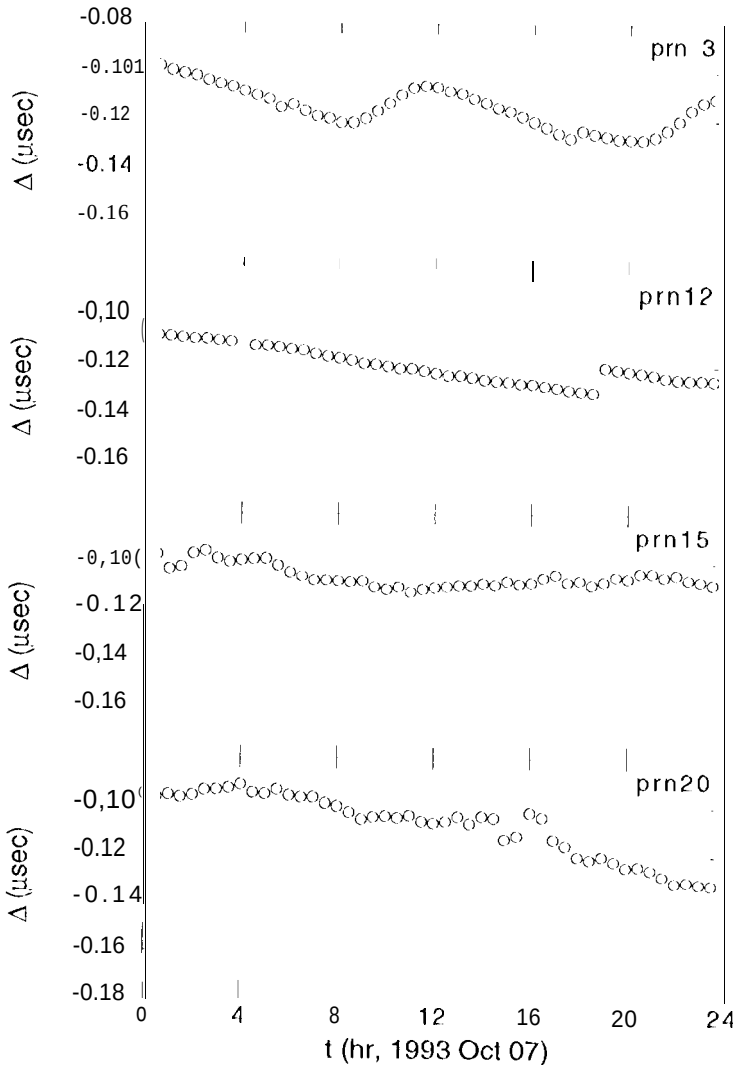

Figure 10 The difference in the broadcast and precise clock corrections, **A**, for 2 Block-Ispacecraft (prns 3 and 12) and two Block-IIspacecraft (prns 15 and 20). Full scale on each plot is 100 ns. The bias of about -120 ns in all of these (as well as that for prn13 in Figure 9) represents a constant difference between GPS reference time and that of the precise solution.

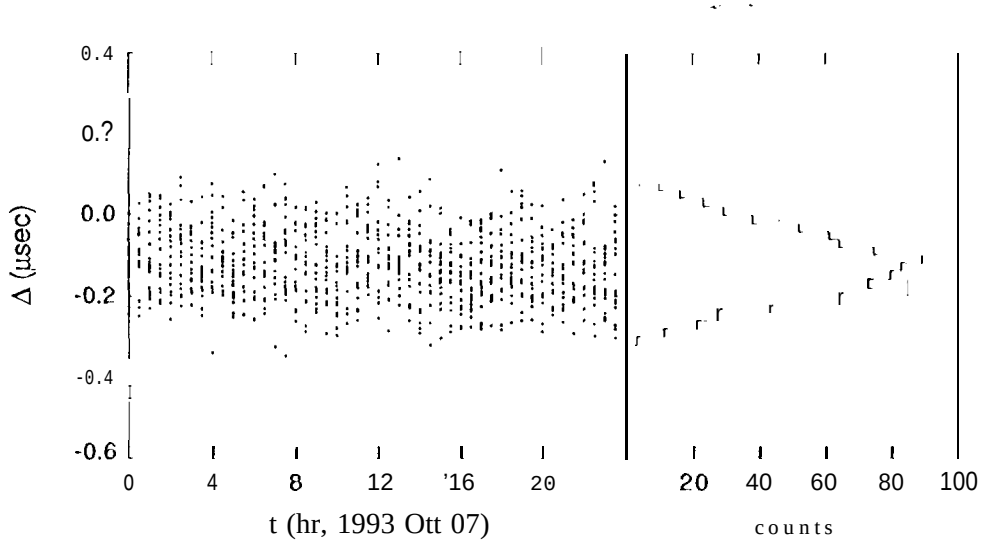

Figure 11 The effects of clock dithering in Selective Availability are shown here, which includes all satellites not shown in Figures 9 or 10. The distribution of **A** (right) has a standard deviation of about 80 ns and a mean of about -120 ns. (The mean is about the same as those in in Figures **9** and 10.)

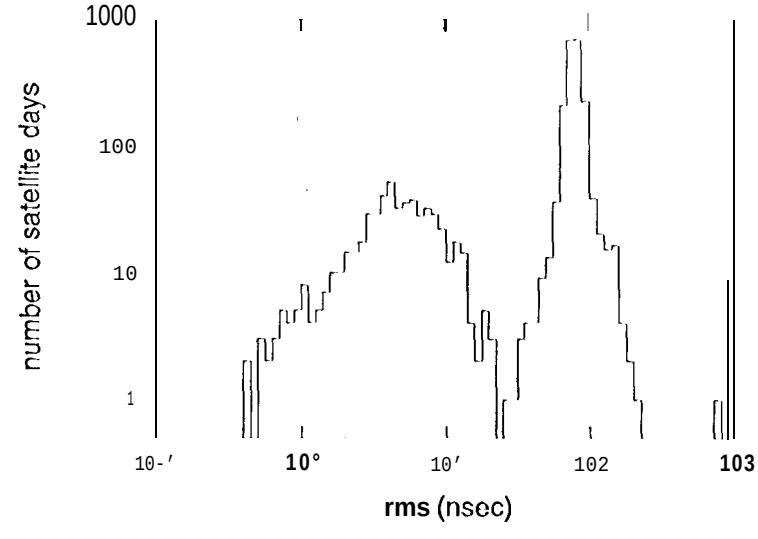

Figure 12 Comparison of broadcast clock solution with precise solut ion, for each day and satellite during the period 1993 Jul 04 through 1993 Ott 22. The bimodal distribution arises from the effects of clock dithering as part of Selective Availability. (There are also a handful of satellites and days when there. was rather poor agreement bet ween the precise solution and the broadcast clock.) The median value of the lower distribution (clock dithering presumably not in effect, rms dc-trended difference over the day between precise solution and broadcast clock Icss than 25 ns) is 4.5 nsec. The median value of the upper distribution is 79.9 nsec.